CHE-14, a protein with a sterol-sensing domain, is required for apical sorting in *C. elegans* ectodermal epithelial cells

Grégoire Michaux, Anne Gansmuller, Colette Hindelang
and Michel Labouesse

Background: Polarised trafficking of proteins is critical for normal expression of the epithelial phenotype, but its genetic control is not understood. The regulatory gene *lin-26* is essential for normal epithelial differentiation in the nematode *Caenorhabditis elegans*. To identify potential effectors of *lin-26*, we characterised mutations that result in *lin-26*-like phenotypes. Here, we report the phenotypic and molecular analysis of one such mutant line, *che-14*.

Results: Mutations in *che-14* resulted in several partially penetrant phenotypes affecting the function of most epithelial or epithelial-like cells of the ectoderm, including the hypodermis, excretory canal, vulva, rectum and several support cells. The defects were generally linked to the accumulation of vesicles or amorphous material near the apical surface, suggesting that secretion was defective. The CHE-14 protein showed similarity to proteins containing sterol-sensing domains, including Dispatched, Patched and NPC1. A fusion protein between full-length CHE-14 and the green fluorescent protein became localised to the apical surface of epithelial cells that require *che-14* function. Deletions that removed the predicted transmembrane domains or extracellular loops of CHE-14 abolished apical localisation and function of the protein.

Conclusions: We propose that CHE-14 is involved in a novel secretory pathway dedicated to the exocytosis of lipid-modified proteins at the apical surface of certain epithelial cells. Our data raise the possibility that the primordial function of proteins containing a sterol-sensing domain is to control vesicle trafficking: CHE-14 and Dispatched in exocytosis, Patched and NPC1 in endocytosis.

Address: Institut de Génétique et de Biologie Moléculaire et Cellulaire, CNRS/INSERM/ULP, BP163, 1 rue Laurent Fries, 67404 Illkirch, France.

Correspondence: Michel Labouesse
E-mail: lmichel@igbmc.u-strasbg.fr

Background

The basolateral and apical membranes of epithelial cells differ in both their protein and lipid contents. For example, the apical domain is enriched in glycosphingolipids while the basolateral domain is enriched in phosphatidylcholine [1]. Differential sorting of proteins at the level of the *trans*-Golgi network (TGN) and polarised secretion are thought to be the primary mechanisms involved in setting this asymmetry [2,3]. Although the sorting determinants responsible for targeting proteins to their final destinations have been fairly well defined, the genetic control of polarised secretion remains poorly understood.

Basolateral sorting determinants often include tyrosine or dileucine residues confined to the cytosolic tails of membrane proteins [4], although other determinants have also been described [5]. In *Caenorhabditis elegans*, basolateral targeting of the epidermal growth factor (EGF) receptor LET-23 requires a complex of the PDZ-domain-containing proteins LIN-2, 7 and 10 [5]. In vertebrates, basolateral targeting can involve a novel clathrin adaptor protein [6] and docking at specific sites in the membrane [3].

Apical sorting determinants may not correspond to simple peptide signals but to specific adducts [2], such as glycosylphosphatidylinositol (GPI) [7], N-glycan [8], O-glycan [9] and possibly even cholesterol [10]. Simons and co-workers have formulated the raft hypothesis, which postulates that the basis for apical sorting is provided by lipid interactions in the form of cholesterol–sphingolipid microdomains [2,11]. These lipid-rich microdomains form in the lumenal leaflet of Golgi membranes [11,12]. Proteins that could mediate apical sorting have been identified on the basis of their enrichment in exocytic vesicles or at apical membranes, their affinity for cholesterol, or in blocking experiments [2]. For example, overexpression of the proteolipid VIP17 (also known as MAL) expands the apical domain, whereas reduction of VIP17 expression impairs transport of several apical markers [13,14]. Formation of apical carriers from the TGN is also inhibited by an anti-annexin XIIIb antibody, whereas it is stimulated by myristoylated recombinant annexin XIIIb [15]. Some of the proteins that mediate docking and fusion with the membrane in the basolateral secretory pathway might also function in apical-directed secretion [2].

Previously, we have shown that mutations affecting the putative transcription factor LIN-26 in *C. elegans* strongly impair the differentiation and function of epithelial-like cells of ectodermal origin, resulting in embryonic or partial larval lethality [16,17]. Ectodermal cells with epithelial characteristics include epidermal cells, and two categories of support cells associated with sensory organs, the sheath and socket cells. Epidermal cells are generally called hypodermal cells because they secrete a collagenous cuticle, which is composed of three main layers (basal, medial and outer cortical). One epidermal cell, the excretory cell, is not covered with cuticle; it extends a long cytoplasmic process called the excretory canal on each side of the animal, and is thought to control osmoregulation [18]. Sheath and socket cells send out a cytoplasmic extension forming a channel at one end, which is likely to correspond to the apical side of the cell as it is where they form an adherens-like junction [19,20]. Both cells are interconnected at the level of this channel, whereas socket cells are connected to the hypodermis and have their channel lined with cuticle in some sensory organs [19,20]. The ciliated endings of sensory neurons access the environment by penetrating the cuticle through the sheath/socket channel. In animals homozygous for the weak mutation *lin-26(n156)*, support cells associated with the amphid and phasmid chemosensory organs accumulate vesicles and are not interconnected, leading to chemosensory defects [16]. When the mutation *lin-26(n156)* is placed in *trans* to a *lin-26* null mutation, *trans*-heterozygous animals do not develop beyond the L2 larval stage, are dumpy, have a defective rectum and often resemble rods that fill with fluid, indicating that osmoregulation is affected [17].

To identify potential *lin-26* effectors, we have looked for mutations with phenotypes similar to those of *lin-26(n156)* mutants. It has previously been shown that in the mutant *che-14(e1960)*, support cells are not interconnected and accumulate vesicles [19], a phenotype that seems reminiscent of that observed in *lin-26(n156)* animals [16]. This similarity raised the possibility that *che-14* could be acting downstream of *lin-26*. Here, we report the characterisation of *che-14* at the phenotypic and molecular levels.

Results
Mutations in *che-14* affect hypodermal and support cells
The mutation *che-14(e1960)* was identified in a screen for mutants defective in dye filling [19]. We obtained three new *che-14* mutations using different approaches (see Materials and methods). The allele *mc16* was isolated through a non-complementation screen against *e1960*; *mc35* was isolated in a clonal screen for mutations displaying *che-14*-like phenotypes; *ok193* was kindly provided by the *C. elegans* knockout consortium subsequent to our cloning of *che-14*, and is likely to be a null allele (see below). All four *che-14* mutations were recessive and could be maintained when homozygous.

All four *che-14* mutants displayed a very similar spectrum of partially penetrant phenotypes. As detailed below, *che-14* mutations affected all epidermal tissues (hypodermis, excretory system, vulva and rectum), causing a partial lethality. Specifically, 5–10% of *che-14* embryos failed to hatch and were partially elongated, with internal cells leaking out of the embryo, which is indicative of a defective hypodermis (Table 1a, Figure 1b). Larval lethality was probably due to an abnormally large and obstructed rectum, leading to constipation (approximately 6% of larvae, see Table 1b, Figure 1d,f), and to an abnormal excretory canal. The excretory defect could account for the approximately 20% of *che-14* animals that died resembling rods filled with fluid (Table 1a, Figure 1h), as all rod-looking animals had an enlarged excretory canal, and the excretory canals of approximately 10% of *che-14* L2 larvae were abnormal (Table 1b, Figure 1j,k). In addition, half of the *che-14* animals that reached adulthood had a variably protruding vulva (Table 1a, Figure 1m,n). Finally, we observed that *che-14* mutants were often slightly dumpy and had a truncated tail spike, which again is indicative of hypodermal defects.

To test whether the amphids and phasmids were normally open to the environment, we used a dye-filling assay similar to the one that led to the identification of *che-14* [19]. In 75% of *che-14* adults, none of the amphid neurons were stained by the lipophilic dye DiO [21], whereas in the remaining mutants (25%) only one amphid was stained (Table 2a). The phasmid staining defect was even more severe (Table 2a). The fact that DiO staining was an all-or-nothing defect suggests that *che-14* affects support cells rather than sensory neurons themselves. To determine the time at which *che-14* is required during development, we observed the evolution of DiO staining at each larval stage. The number of stained amphid neurons was almost normal in L1 larvae and decreased after the L1–L2 moult (more rapidly in *e1960* than in *ok193*, see Table 2b), indicating that *che-14* is necessary for maintaining a process rather than for establishing it. In summary, *che-14* mutations affect all hypodermal organs and the amphid/phasmid support cells, in a manner quite similar to the allele *lin-26(n156)*. The molecular link between *lin-26* and *che-14* will be addressed in a separate study.

Apical abnormalities and secretory defects in *che-14* mutants
When the bodies of *mc35* and *ok193* adults were examined by transmission electron microscopy (two control animals did not show any of the defects discussed below), three classes of excretory canal defects were observed (Figure 2b,c,f). First, it was not properly attached to the basement membrane in two out of four *mc35* canals and two out of seven *ok193* canals (a canal could not be found in one *ok193* mutant). Second, the lumen was abnormally open in three out of seven *ok193* canals (but none in *mc35*). Third, its transverse section was larger than normal

Table 1

**Phenotypic characterisation of *che-14* mutants.**

(a) Genotype	Dead eggs*	Rods†	Pvl adults‡	Other§	n
Wild type	<1%	0%	<1%	>99%	446
che-14(e1960)	6%	21%	27%	46%	242
che-14(mc35)	13%	19%	35%	33%	246
che-14(mc16) unc-29(e1072)¶	9%	15%	34%	42%	234
che-14(ok193)	5%	27%	25%	43%	355
che14(ok193) + pML624¥	2%	2%	<1%	>95%	116

(b) Genotype	Thick excretory canal**	Constipated††	Vacuoles§§	Wild type	n
Wild type	0%	0%	0%	100%	112
che-14(e1960)	9%	8%	10%	84%	128
che-14(mc35)	13%	4%	9%	87%	116
che-14(mc16) unc-29(e1072)	10%	8%	8%	84%	116
che-14(ok193)	7%	4%	8%	85%	118

(a) Terminal phenotypes of animals and **(b)** cellular defects in L2 larvae with the indicated genotype for *n* scored animals. *Eggs that failed to hatch (see Figure 1b). †Larvae and adults displaying rod-like lethality (see Figure 1h). ‡Adults with a protruding vulva (see Figure 1m,n). §*che-14* adults with a normal vulva. ¶*unc-29(e1072)* animals displayed none of these phenotypes on their own. ¥Plasmid pML624 expresses full-length CHE-14 fused to the green fluorescent protein (CHE-14–GFP). Expression of this fusion protein rescued the

che-14 mutation. In (b), because different phenotypes could be observed in the same larva, the total can exceed 100%. **Larvae with an enlarged excretory canal (see Figure 1j,k). When the excretory canal was enlarged, a vacuole was present in the excretory cell body and/or in the duct. ††Larvae with accumulation of food in the terminal part of the intestine and with a defective rectum (see Figure 1d,f). §§Larvae displaying a rod-like phenotype (Figure 1h) or with widespread vacuoles in their hypodermis.

in three out of four *mc35* canals (but normal in *ok193*). Failure to attach to the basement membrane has previously been linked to apical defects [22]. In hypodermal cells, the two outer layers of the cuticle in *ok193* and *mc35* animals appeared overall half as thick as in control animals, while the most basal layer had an irregular thickness, as has previously been reported for head hypodermis in *e1960* animals [19]. This defect was particularly prominent in the lateral row of hypodermal cells called the seam cells, which secrete a protruding cuticular ridge

called the alae. In *ok193* and *mc35* adults, the alae were strongly altered and the most basal layer of the cuticle was twice as large as in control adults (Figure 2e,f; see also Figure 3f,g). In some sections, large deposits of amorphous material could be found between the cuticle and the seam cytoplasm (Figure 2e). The abnormal accumulation of material at the apical membrane together with the thinner cuticle and alae suggest that the two are linked, and that *che-14* is required for the secretion of proteins that should be incorporated into the cuticle.
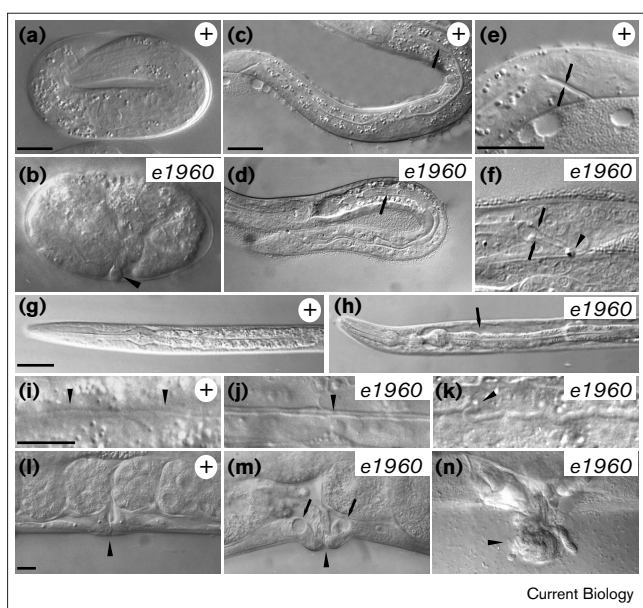
Similarly, to extend the observations made by Perkins and co-workers [19], we examined sections at different levels in the heads of *mc16*, *mc35* and *ok193* adults (four control

Current Biology

Figure 1

The *che-14(e1960)* mutation affects various hypodermal cells. Nomarski micrographs of **(a,c,e,g,i,l)** wild-type (+) or **(b,d,f,h,j,k,m,n)** *che-14(e1960)* animals at different stages. (a,b) Terminal-stage embryos. The *che-14* embryo in (b) failed to elongate and some internal cells were leaking out (arrowhead). (c,d) Intestine (arrow). (e,f) Enlargement of the rectum (double arrow) in (f) *che-14* L2 larvae; in this *che-14* mutant, the intestine was filled with food because of an obstructed rectum (arrowhead). (g,h) L2 larvae. The *che-14* larva in (h) displayed a characteristic rod-like lethality, with a fluid-filled body cavity (arrow). (i–k) Higher-magnification views of the excretory canal in L2 larvae (arrowheads). In the mutants shown in (j,k), the excretory canal was enlarged and (j) linear or (k) meandering. The animal in (j) was a rod. (l–n) Adult vulva (arrowhead). The vulva of *che-14* adults could be normal, (m) slightly protruding or (n) completely everted. Vacuoles (arrow) were occasionally present in the vulva as in other hypodermal tissues. Anterior is to the left, dorsal is uppermost. The scale bar represents 10 μm.

Table 2

The *che-14* mutants fail to stain with DiO.

(a)

Genotype		Amphid staining				Phasmid staining			
	n	Number of cells*	Two sides[†]	One side[†]	No staining	Number of cells*	Two sides[†]	One side[†]	No staining
Wild type	50	11.7 ± 0.6	100%	0%	0%	4 ± 0	100%	0%	0%
che-14(e1960)	50	1 ± 2	0%	22%	78%	0 ± 0	0%	0%	100%
che-14(mc35)	50	1 ± 1.7	0%	26%	74%	0 ± 0	0%	0%	100%
che-14(mc16) unc-29(e1072)[‡]	50	1.3 ± 2.2	0%	26%	74%	0.26 ± 0.9	4%	6%	90%
che-14(ok193)	50	1.5 ± 2.3	2%	24%	74%	0 ± 0	0%	0%	100%
che-14(e1960) + M01E4[§]	20	11 ± 1.3	95%	5%	0%	3.7 ± 0.7	85%	15%	0%
che-14(e1960) + pML624[¶]	15	10.8 ± 2.5	80%	20%	0%	2.5 ± 1.6	45%	35%	20%

(b)

Genotype		Amphid staining					Phasmid staining				
	n	L1	L2	L3	L4	Adult	L1	L2	L3	L4	Adult
Wild type	50	9 ± 0.9	9.4 ± 0.8	9.8 ± 0.9	11.3 ± 0.8	11.7 ± 0.6	1 ± 1	3.3 ± 0.8	4 ± 0	4 ± 0	4 ± 0
che-14(e1960)	50	7.6 ± 2.3	1.7 ± 3	0.6 ± 1.5	0.3 ± 1.2	1 ± 2	0 ± 0	0.1 ± 0.4	0 ± 0	0 ± 0	0 ± 0
che-14(ok193)	50	6.8 ± 2.7	5.1 ± 3.5	3.2 ± 2.9	2.2 ± 2.4	1.5 ± 2.3	0.2 ± 0.5	0.3 ± 0.6	0.2 ± 0.6	0 ± 0	0 ± 0

(a) DiO staining of amphid and phasmid neurons in adults. *Total number of stained cells (± SD) for *n*-scored animals. Amphids and phasmids are bilateral organs; six neurons per amphid and two per phasmid can fill with DiO. [†]Percentages correspond to stained organs. An organ was considered to be stained if at least half of its neurons were stained. Two sides, worms in which both amphids or phasmids were stained; one side, only one amphid or phasmid were stained. [‡]*unc-29(e1072)* animals displayed normal DiO staining on their own. [§]*M01E4* is a rescuing cosmid. [¶]Plasmid pML624 expresses CHE-14–GFP and rescues *che-14* mutants. **(b)** Average number of stained neurons per animal during larval development.

animals did not show any of the defects discussed below). We observed that the amphid socket cell either failed to form a channel (one out of four socket cells in *mc35* animals), or it formed a channel filled with dark electron-dense material (two out of two *mc16* sockets; three out of four *mc35* sockets; four out of four *ok193* sockets) in which the neuronal terminal dendrites were not visible (Figure 3b–d; they were partially visible in one of four *mc35* sockets). More posteriorly, the amphid sheath cell accumulated numerous vesicles and failed to form a normal channel (none out of two *mc16* sheaths, one out of four *mc35* sheaths and none out of four *ok193* sheaths were normal; Figure 3f,g), preventing normal morphogenesis of chemosensory ciliated endings. These vesicles could correspond to the matrix material that is normally secreted by the sheath cell into the channel [19]. In some cases, the vesicles fused and resulted in the formation of a large pocket of matrix-like material (Figure 3d). The anterior-most parts of the channels associated with other sensory organs (cephalic, outer and inner labial) were generally filled with matrix material in *ok193* adults (two animals), as described above for the amphid, but were essentially normal in *mc16* and *mc35* adults (data not shown). In conclusion, these ultrastructural studies are consistent with Nomarski and DiO staining defects described above. They suggest that, in both the hypodermis and the amphid support cells, *che-14* is required for a secretory process and primarily affects structures found at the apical side of these cells.

The *che-14* gene encodes a protein with a sterol-sensing domain

We cloned *che-14* by complementation rescue of the dye-filling defect of *e1960* animals and found that it corresponds to the predicted gene *F56H1.1* (Figure 4a). Comparison between the genomic sequence and two cDNAs showed that *che-14* contains 18 exons, spanning approximately 8 kb. We confirmed that *che-14* is *F56H1.1* by sequencing the four *che-14* alleles (Figure 4a; see Supplementary material for further details). We found that *ok193* deletes 3 kb within *che-14* and is most likely a null mutation as the deletion encompasses the fifth to the penultimate exon; *mc35* is a small deletion associated with a 3 kb insertion; *mc16* and *e1960* affect splice donor sites, resulting in aberrant transcripts (data not shown) that lead to premature translation termination.

Database searches showed that the 917 amino acid long CHE-14 protein is most similar to three proteins thought to have 12 transmembrane segments, Dispatched (Disp), Patched (Ptc) and NPC1 (the similarity was slightly higher to Disp; see Supplementary material). Disp is a *Drosophila* protein dedicated to the release of cholesterol-modified Hedgehog (Hh) from signalling cells [23]. The *Ptc* gene is a segment-polarity gene in *Drosophila*, thought to encode the Hh receptor [24,25]. NPC1 is responsible for Niemann–Pick disease type C1 [26], a progressive neurodegenerative disorder characterised by lysosomal sequestration of endocytosed low-density lipoprotein

Figure 2
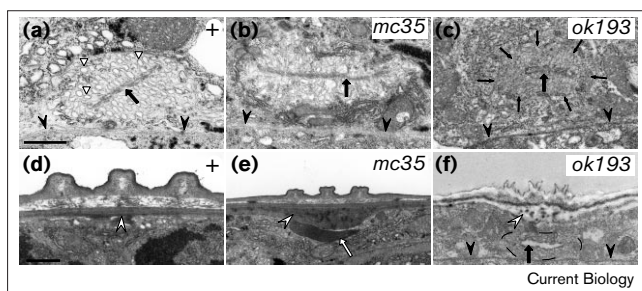
Mutations in *che-14* affect the cuticle and the excretory canal. Transmission electron micrographs of **(a,d)** wild-type, **(b,e)** *che-14(mc35)* and **(c,f)** *che-14(ok193)* adults. (a–c) Transverse sections through the excretory canal. The outline of the canal is indicated by thin arrows in (c). In both *che-14* mutants, the excretory canal had detached from the basement membrane (arrowheads); in the *mc35* animal, the lumen of the excretory canal (arrow) was longer. Canaliculi within mutant canals generally appeared normal (compare with the wild type; small unshaded arrowheads in panel a). (d–f) Transverse sections through the cuticle at the level of the anterior gonad arm. The alae and outer layers of the cuticle appeared thinner in (e,f) *che-14* mutants, and the basal layer of the cuticle was enlarged (arrowheads). (e) Amorphous material had accumulated in the *mc35* mutant (arrow). (f) The excretory canal, which is positioned under the alae in this *ok193* mutant, had its lumen open (arrow); the outline of the canal is indicated with a dashed line). The scale bar represents 500 nm.

(LDL)–cholesterol [27]. The hydrophobic plot of CHE-14 predicted at least 12 hydrophobic peaks and was quite similar to that of Disp (Figure 4b,c), Ptc and NPC1 (data not shown). It has previously been noticed that Disp, Ptc and NPC1 have significant homology with the sterol-sensing domain found in HMG-CoA reductase [28] and SCAP [29], two proteins implicated in cholesterol home-ostasis. Consistent with the extended similarity observed between CHE-14 and Disp, a putative sterol-sensing domain was found in CHE-14, suggesting that it might bind sterol-modified proteins. CHE-14 also shows high similarity to F07C3.1, a *C. elegans* protein of unknown function, and to a protein deduced from the sequence of a partial cDNA encoding the putative human Disp ortho-logue. For the latter, the similarity was prominent in the last five transmembrane domains of CHE-14 (see Supple-mentary material).

CHE-14 is found at the apical membrane of epithelial cells in the ectoderm

To gain further insights into CHE-14 function, we exam-ined its expression pattern and subcellular localisation using a construct encoding GFP, fused immediately before the *che-14* stop codon. The CHE-14–GFP fusion protein rescued the partial lethality (Table 1a) and the dye-filling defect (Table 2a) of *che-14* mutants. In wild-type animals, GFP fluorescence was observed in all hypodermal cells (Figure 5a–p) and support cells (Figure 5q,r), starting at

mid-embryogenesis (comma stage). Expression was stronger in the lateral seam cells (Figure 5a–h), excretory system (Figure 5i–l), vulva (Figure 5m,n) and rectum (Figure 5o,p). The CHE-14–GFP fusion protein was enriched at the apical surface in hypodermal cells (Figure 5b,f,l,n,p) or in the equivalent area where support cells form a channel (Figure 5r), but could also be detected at low levels in the cytoplasm, where it often looked punctate (Figure 5d,h,r). To summarise, the CHE-14–GFP fusion protein was found in cells and at the subcellular domain that were affected by *che-14* mutations; as this fusion protein could rescue *che-14* defects, it suggests that *che-14* acts cell autonomously.

CHE-14 deletion analysis

To identify important functional domains in CHE-14, we deleted parts of each predicted extracellular loop, trans-membrane segments, or three distinct and adjacent seg-ments encompassing the last 29 amino acids, which are predicted to be cytoplasmic (Figure 6a). These deletion constructs were all properly expressed as evidenced from the normal levels of GFP autofluorescence, showing that the deleted sequences were not important for expression. Except for carboxy-terminal deletions, all other deletions affected the subcellular localisation of the fusion protein, which remained cytoplasmic instead of apical (Figure 6b–g), and abolished its ability to rescue the dye-filling defect of *che-14(e1960)* animals (Figure 6a). We conclude that the predicted extracellular loops and transmembrane seg-ments are essential for CHE-14 localisation and possibly for its function, but that the cytoplasmic carboxy-terminal tail is apparently dispensable.

Discussion

We have characterised the *C. elegans che-14* gene and found that it is involved in secretion towards the apical surface of epithelial cells; *che-14* mutations are the first to be described that affect apical sorting in epithelial cells. Transmission electron microscopy showed that the two external layers of the cuticle in *che-14* mutants were approx-imately half as thick as normal. The basal layer was enlarged, and dark amorphous material accumulated imme-diately under the cuticle. This defect strongly suggests that material that should have been secreted apically remained trapped inside the cell, preventing normal function of these cells. Consistent with a function in apical sorting and secre-tion, CHE-14 is a multipass transmembrane protein with a putative sterol-sensing domain and is enriched at the apical surface of epithelial-like cells of the ectoderm.

The *che-14* mutants also accumulated vesicles in sheath cells, as do many other dye-filling negative mutants [19]. Because mutations that genetically act in neurons rather than in support cells display this defect, it has been sug-gested that it may be indirect [30] and linked to the fact that cilia probably stimulate the secretion of matrix by sheath cells [19]. Although we cannot rule out an indirect

Figure 3

Mutations in *che-14* affect sensory organ support cells. Transmission electron micrographs of **(a,c,e)** wild-type, **(b,f)** *che-14(mc35)* and **(d,g)** *che-14(ok193)* adults. The sections were taken from the same *che-14* mutant in (b,f) and in (d,g), respectively. (a,b) Transverse section through the amphid socket channel, approximately 1.3 µm from the nose. (a) In the wild type, the exposed amphid sensory endings (white arrowheads) run through the socket channel (black arrowhead). (b) Dark material accumulated in this *mc35* mutant where the socket channel should be (black arrowhead). (c,d) Transverse section at the level of the amphid socket–sheath junction, approximately 3 µm from the nose. (d) Both socket channels were obstructed (arrowheads) in this *ok193* mutant; a large deposit of dark matrix-like material was also visible in the sheath cell (arrow). (e–g) Sections posterior to the socket–sheath junction, approximately 6 µm from the nose. (e) Note in the control animal the sensory endings of exposed amphid neurons (large white arrowheads) and the numerous fingers of the AFD neuron, which is responsible for thermotaxis behaviour (small arrowheads); these dendrites are separated by matrix material in the sheath channel. (f) In the *mc35* mutant, several dark vesicles were visible (black arrows). The number of sensory


Current Biology
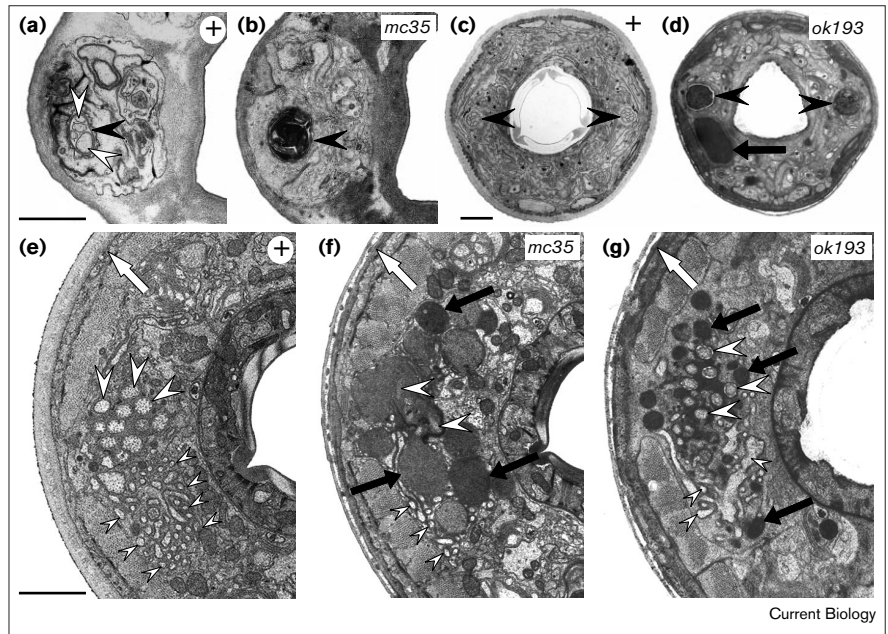
endings was reduced both for normally exposed neurons (white arrowheads; one was deflected laterally) and the AFD neuron (small arrowheads). (g) Similarly, in the *ok193* mutant, there were dark vesicles (black

arrowheads) and the number of dendrites was reduced; those that were visible were abnormal. The head cuticle appeared thinner in both *che-14* mutants (white arrow). The scale bar represents 1 µm.

effect, we believe that vesicle accumulation in *che-14* mutants is directly linked to defective secretion. First, *che-14* mutations are the only ones (together with *lin-26(n156)*, [16]) to induce the accumulation of so many or so large vesicles ([19], and Figure 3). Second, our

experiments with the CHE-14–GFP fusion protein suggest that *che-14* acts cell autonomously within support cells. In other words, we suggest that vesicle accumulation can be due to the absence of cilia (as in cilium-assembly mutants) or to sheath-cell defects (as in *che-14* and *lin-26*
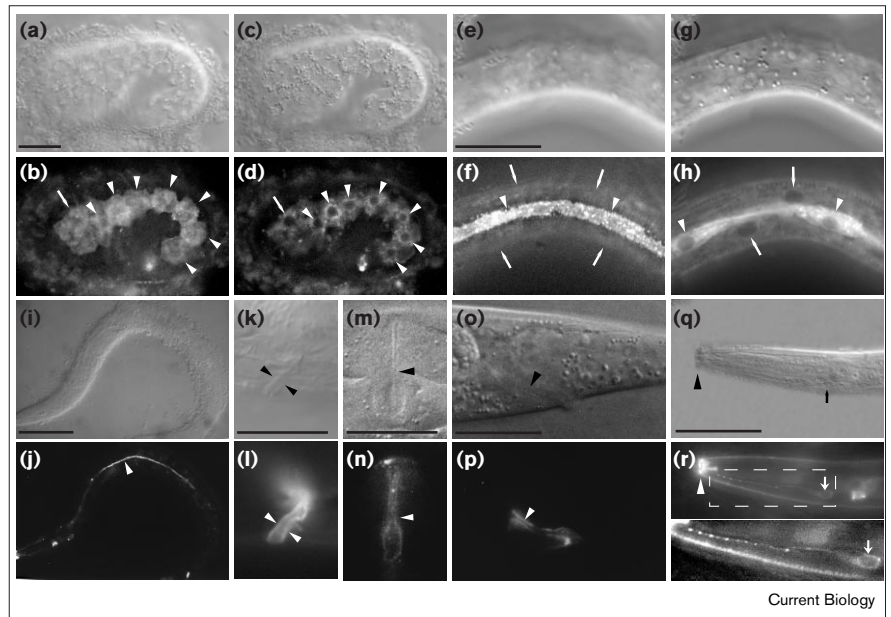
Figure 4

Current Biology
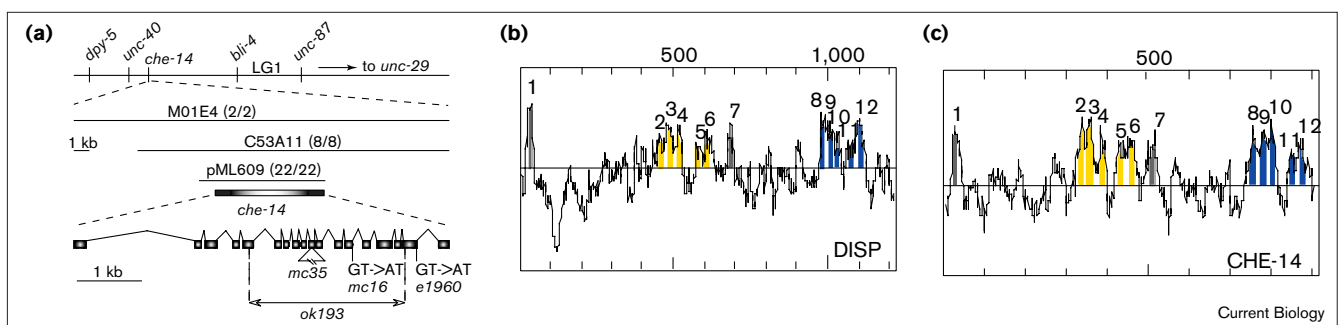
The *che-14* gene encodes a protein containing a sterol-sensing domain, with homology to Disp. **(a)** Cloning of *che-14*. A portion of linkage group I (LG1) is shown; *che-14* maps close to *unc-40*. The rescuing cosmids *M01E4* and *C53A11*, and a genomic map of *che-14* are shown under the genetic map. The numbers of lines in which the dye-filling defect of *che-14(e1960)* was rescued are indicated in parentheses for each cosmid/plasmid. The *ok193*, *mc35*, *mc16* and *e1960* are indicated: *ok193* is a deletion removing the sequences delineated by the

double-arrow; *mc35* is a small deletion accompanied by an insertion (triangle); *mc16* and *e1960* are splice mutations. **(b,c)** Hydrophobic plots of Disp and CHE-14 generated using the algorithm of Kyte and Doolittle [46]. The numbers indicate hydrophobic segments that are likely to be transmembrane segments, and the colour code corresponds to the conserved domains: yellow, putative SSD; blue, Ct domain (see Supplementary material).

Figure 5

The *che-14* gene is expressed in epithelial cells of the ectoderm. Nomarski and corresponding fluorescence images in the same focal plane of wild-type animals expressing CHE-14–GFP. **(a,b,e,f)** Apical focal plane and **(c,d,g,h)** deeper focal plane at the level of the nuclei in (a–d) a 1.5-fold-stage embryo and (e–h) an L2 larva, focusing on the hypodermis. The fusion protein was absent from the basolateral membrane, abundant at the apical membrane and slightly punctate in the cytoplasm. It was particularly abundant in seam cells (white arrowheads) but also visible in other hypodermal cells (white arrows). **(i,j)** Excretory canal in an L1 larva. Views of the **(k,l)** excretory pore, **(m,n)** vulva and **(o,p)** rectum in an adult, and **(q,r)** head support cell in an L2 larva. In each case, the fusion protein was mainly detected on the apical side of cells, either facing the lumen of the excretory pore, vulva and rectum (arrowheads), or at the position where support cells form a channel (arrowhead). The inset in (r) shows an enlargement of the region boxed with a dashed line, showing the cell body (arrow) and cytoplasmic extension of a cell that was tentatively identified as the IlshVR. Not all sheath and socket cells expressed the fusion protein. This was due, at least in part, to mosaicism [44]. Anterior is to the left and dorsal is uppermost. The scale bar represents 10 μm.

mutants). Importantly, our conclusions are based on the analysis of four mutations that appear to affect development in a similar way. One of them, *ok193*, is most likely a null mutation. The other three (*e1960*, *mc16* and *mc35*) truncate CHE-14 after the sterol-sensing domain and may not completely eliminate *che-14* function. Indeed, the ultrastructural defects observed in *mc35* mutants were slightly less penetrant than in *ok193* mutants. In addition, the *e1960* allele may have a neomorphic activity, as it caused slightly more severe dye-filling defects in young larvae than *ok193*.

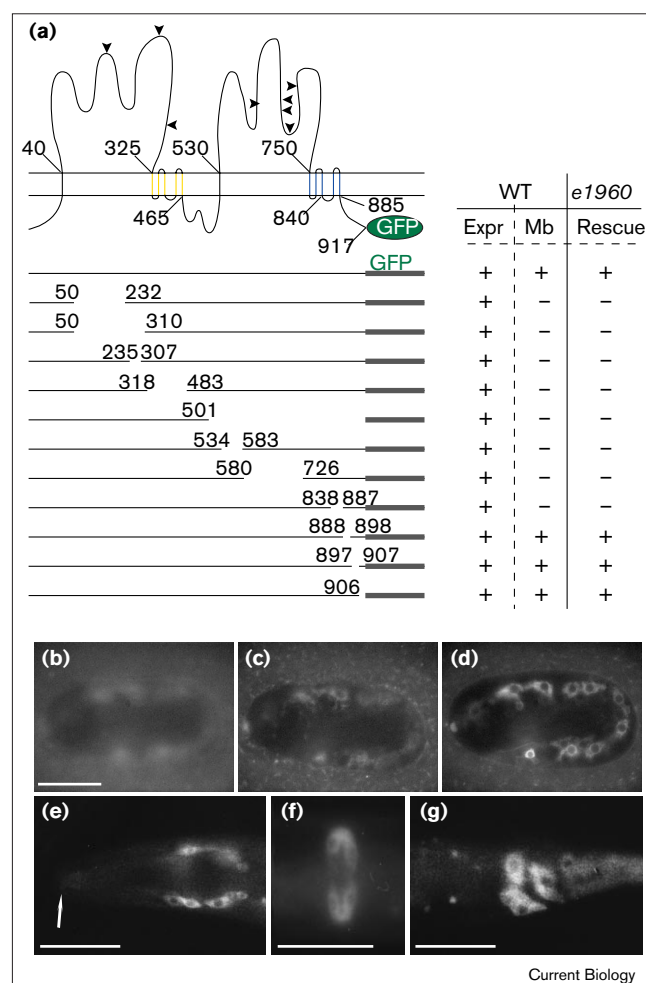**CHE-14 acts at a late step during apical sorting**

A striking feature of *che-14* mutants was that their phenotypes (embryonic lethality, protruding vulva, obstructed rectum, excretory canal defects) were not 100% penetrant, even in animals homozygous for the null allele *ok193*. In addition, the dye-filling defect, which was severe in adults, hardly affected young *che-14* larvae, indicating that amphid sensory organs were initially functional. At least two mutually non-exclusive possibilities could account for these observations. The *che-14* gene product could be functioning in the secretion of certain stage-specific and/or non-essential proteins. If *che-14* had been required for trafficking of all apical proteins, we would have expected an embryonic lethal phenotype associated with a loss of epithelial polarity or integrity (similar, for instance, to what is observed in *let-413* mutants [31]), whereas less than 10% of *che-14* embryos had potentially such defects.

The presence of a putative sterol-sensing domain in CHE-14 raises the possibility that it is specifically required to secrete proteins containing sterol or GPI adducts. Such proteins might be required, for instance, after the L1 stage in support cells, and might be components of the outer cuticle. A major goal in the future will be to identify proteins that require *che-14* activity for secretion. Alternatively, *che-14* could act redundantly with genes that compensate for its loss and allow morphogenesis of the vulva, rectum and excretory canal to proceed normally (as seen in many *che-14* animals). One such gene could be *F07C3.1*, which shows strong similarity to *che-14*. We tested this possibility by performing RNA interference against *F07C3.1* in wild-type or *che-14* backgrounds, but did not observe any phenotype compared with controls (data not shown). On the basis of the subcellular localisation of CHE-14 and from the observation that vesicles or amorphous material accumulate under the apical membrane rather than anywhere else in the cell, we suggest that CHE-14 controls a late step during the process of apical protein sorting. As CHE-14 was also detected in the cytoplasm, often in a punctate pattern, it may assemble with secretory vesicles at the level of the TGN.

It has been proposed that lipid microdomains provide the biochemical basis for apical sorting in epithelial cells [2,11]. With respect to this model, it is tempting to speculate that CHE-14, with its potential sterol-sensing domain, might be a component of lipid rafts. To assess this possibility, we

Figure 6

CHE-14 deletion analysis. **(a)** Predicted topology of the CHE-14–GFP fusion protein (see Supplementary material). The numbers correspond to amino acids and indicate the beginning or end of transmembrane segments; arrowheads correspond to potential N-glycosylation sites. The other symbols are as in Figure 4. Each of the lines below represents a different plasmid construct ending with sequences encoding GFP; numbers indicate amino-acid positions at the limits of each deletion. Each construct was injected into wild-type (WT) and *che-14(e1960)* animals and the results are shown on the right. Expr, expression; mb, apical-membrane localisation in wild-type animals; rescue, rescue of the dye-filling defect. **(b–g)** A few examples of localisation patterns seen with the deletion constructs. All non-rescuing constructs had the same subcellular localisation. (b–d) Expression in a two-fold-stage embryo of CHE-14 carrying a deletion between amino acids 534–583. (b) Apical focal plane through seam cells. (c) Sub-apical focal plane and (d) nuclear focal plane through the hypodermis. The fusion protein was no longer detected at the apical membrane (compare with Figure 5a–d). (e–g) Expression in adults of CHE-14 carrying a deletion between amino acids 50–232. (e) Head support cells. (f) Vulva. (g) Rectum. The fusion protein was only visible in the cytoplasm (compare with Figure 5m–r). In (e), note that there was no staining at the tip of the nose (arrow). Anterior is to the left and dorsal is uppermost. The scale bars represent 10 µm.

construct	WT Expr	WT Mb	e1960 Rescue
GFP (917)	+	+	+
50 – 232	+	–	–
50 – 310	+	–	–
235 – 307	+	–	–
318 – 483	+	–	–
501	+	–	–
534 – 583	+	–	–
580 – 726	+	–	–
838 – 887	+	–	–
888 – 898	+	+	+
897 – 907	+	+	+
906	+	+	+

examined whether *che-14* mutations would synergise in some way with an inactivation of the genes for two putative *C. elegans* raft components, the caveolin homologues CAV-1 and CAV-2. *cav-1* is expressed in epithelia but does not appear to be essential in the ectoderm [32]. Inhibiting the expression of *cav-1* and *cav-2*, alone or in combination, in a *che-14* background using RNA interference did not result in new phenotypes, indicating that *che-14* does not act redundantly with these two genes. Future work will need to establish whether CHE-14 is a raft component. Meanwhile, our efforts to delineate important functional domains within CHE-14 have indicated that the two suggested extracellular loops are essential for apical localisation. As it is known that N- and O-glycosylation can provide apical-sorting signals [8,9], deletions within the extracellular loops might eliminate key residues that should be glycosylated to target CHE-14 apically.

Very few mutations are known in *C. elegans* that directly or indirectly affect cholesterol homeostasis. Mutations in *lrp-1*, which encodes a gp330/megalin-related protein necessary for cholesterol endocytosis, result in an inability to shed and degrade the old cuticle at each larval moult [33]. Mutations affecting the two *C. elegans* NPC1 homologues result in premature egg-laying, hypersensitivity to cholesterol deprivation and a dauer-constitutive phenotype [34]. The fact that we did not observe such defects in *che-14* mutants (see above; data not shown) reinforces the conclusion that *che-14* affects exocytosis rather than endocytosis.

Implication for sterol-sensing domain proteins

Sequence comparison showed that CHE-14 is similar to Disp and Ptc, which are involved in Hh signalling, raising the possibility that *che-14* might be involved in a Hh signalling pathway. Homologues of Hh and most other components of the Hh signalling pathway [35] have not been identified in *C. elegans* [36]. For this reason, we do not think that *che-14* is involved in a Hh signalling pathway. In addition, the first *C. elegans* Ptc homologue to be described appears to function in germ-line cytokinesis, a process in which *che-14* is not involved [37]. Conversely, we suggest that the sequence similarities between CHE-14, Disp, Ptc and NPC1, as well as some common features of their loss-of-function phenotypes, reveal the primordial function of these proteins. As discussed above, we suggest that *che-14* is required for a late step in a secretory pathway dedicated to the exocytosis of sterol-modified proteins. Disp is required for the release of HhN (the Hh form generated after auto-proteolytic cleavage and addition of cholesterol [10]) by a mechanism that has not been analysed at the subcellular or biochemical levels. As Disp is more closely related to CHE-14 (see Supplementary material), it might act in a secretory pathway involved in the exocytosis of HhN-containing vesicles. As Ptc is more related to NPC1, which has clearly been implicated in vesicle trafficking between late endosomes and lysosomes [26,27], and as it is found both at the apical membrane in *Drosophila* imaginal disc and in endosomes [38], its primary

Figure 7
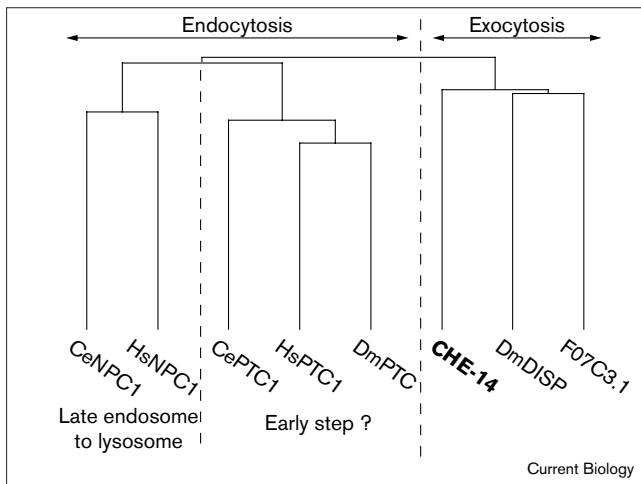
A model for the function of proteins containing sterol-sensing domains. Dendrogram of proteins containing sterol-sensing domains. Proteins belonging to the same branch are also likely to be related by function (for further details, see text).

function could be to endocytose Hh. In summary, we suggest that proteins in the CHE-14/Disp branch are required for exocytosis, whereas proteins in the NPC1/Ptc are required for endocytosis perhaps at different steps in the endocytotic pathway (see Figure 7).

Materials and methods
Strains and general methods
C. elegans strains were maintained at 20°C under standard conditions [39]. The Bristol strain N2 was the reference strain. The following mutations were used: *che-14(e1960)* [19]; *dpy-5(e61)*; *unc-40(e271)*; *bli-4(e937)*; *unc-29(e1072)* [39]; *unc-87(e1216)* [40]; *him-5(e1490)* [41].

Isolation and characterisation of che-14 alleles
The allele *che-14(mc16)* was identified in a non-complementation screen against *e1960*. Briefly, *unc-29; him-5* males were mutagenised with ethyl methane sulphonate [39], crossed with *dpy-5(e61) che-14(e1960)* hermaphrodites, and the cross-progeny were examined for dye-filling defects (see below). We found one new *che-14* allele, *mc16*, among 5670 non-Dpy F1 hermaphrodites. The allele *che-14(mc35)* was isolated after trimethylpsoralen mutagenesis [42] in a clonal screen for mutants displaying partial rod-like lethality and dye-filling defects similar to those observed in *e1960* and *mc16* animals; 6500 F1 mutagenised animals were singled out onto individual plates and their progeny were inspected for the presence of rod-like dead larvae. F1 animals segregating rods were subsequently stained with DiO. The allele *che-14(ok193)* was provided by the *C. elegans* Knockout Consortium after trimethylpsoralen mutagenesis. It was identified by nested PCR using primers located 4.2 kb apart within *che-14*. The alleles *mc35* and *ok193* were outcrossed six times with N2 (four times for *mc16*).

To assess the viability of *che-14* mutants, 10–20 homozygous *che-14* hermaphrodites were allowed to lay eggs for 2–4 h, and their progeny were examined at each developmental stage. Similarly synchronised L2 larvae were examined by Nomarski optics for cellular defects. Dye-filling assays were performed at each developmental stage using 3,3′-dioctadecyloxacarbocyanine perchlorate (DiO) [16,21]. For electron microscopy, animals were prepared as described elsewhere [16,43]. The defects described in the text correspond to defects consistently observed in several adjacent sections. One *mc16*, two *mc35*, two *ok193* and four N2 animals were sectioned in the nose; two *mc35*, four *ok193* and two N2 animals were sectioned in the body.

Identification of che-14
The *che-14* locus had been mapped between *dpy-5* and *unc-13* on linkage group I [19]. Further mapping positioned it at approximately 0.04 map units to the right of *unc-40*. Starting from *dpy-5+ unc-87/+ che-14(e1960)+* animals, 5/19 Dpy non-Unc and 8/9 Unc non-Dpy animals segregated *che-14* animals; starting from *unc-40+ bli-4/+ che-14(e1960)+* animals, 29/31 Bli non-Unc segregated *che-14* animals. To clone *che-14*, cosmids from the *unc-40* region were injected in *che-14(e1960)* animals using pRF4 [*rol-6(su1006)*] as a co-injection marker [44]. Cosmids *M01E4*, *F56H1*, *C53A11* and a 9 kb *EcoRI* fragment from *F56H1* (GenBank accession number AF067618) carrying only *F56H1.1* (plasmid pNL609) could rescue the dye-filling defect of *che-14(e1960)* animals. Northern blots were performed using RNA isolated from N2 animals. The 2.7 kb cDNA yk354g7 provided by Y. Kohara was sequenced. A 200 bp fragment corresponding to the putative 5′ part of *che-14* was cloned by RT–PCR and added to yk354g7 to give pML650. To identify *che-14* mutations, DNA fragments spanning each exon were amplified from mutants animals and sequenced on both strands. The accession number for the cDNA cloned into pML650 is AJ277649.

CHE–GFP expression pattern and CHE-14 deletion analysis
The rescue plasmid pML624 was constructed as follows: a 9 kb fragment containing the upstream regulatory sequences necessary for rescue and the coding region up to the last codon was amplified by long-range PCR (Expand™, Boehringer) from *F56H1* and cloned in frame with the GFP coding sequence [45] between the *BamHI* and *KpnI* sites of pPD95.75 (kind gift from A. Fire). Deletion analysis of CHE-14 was made by either of two methods. Some constructs were generated by religation of pML624 after cleavage with two restriction enzymes and treatment with Klenow enzyme (*EcoRV* and *PmlI*, *EcoRV* and *XcmI*, *PmlI* and *XcmI*). Other constructs were generated by long-range PCR using primers with a built-in *MluI* site designed to amplify most of pML624 except a small fragment (presence of the *MluI* site results in the insertion of Thr and Arg residues in the protein). All constructs for expression of GFP were injected at 20 ng/μl and 3–5 independent lines were examined by fluorescence and Nomarski optics. Whenever possible, several independent plasmid clones for a given construct were used to look at the expression pattern. The sequences of primers used in this study are available on request.

References
1. Simons K, van Meer G: **Lipid sorting in epithelial cells.** *Biochemistry* 1988, **27**:6197-6202.
2. Ikonen E, Simons K: **Protein and lipid sorting from the *trans*-Golgi network to the plasma membrane in polarized cells.** *Semin Cell Dev Biol* 1998, **9**:503-509.
3. Yeaman C, Grindstaff KK, Nelson WJ: **New perspectives on mechanisms involved in generating epithelial cell polarity.** *Physiol Rev* 1999, **79**:73-98.
4. Mellman I: **Endocytosis and molecular sorting.** *Annu Rev Cell Dev Biol* 1996, **12**:575-625.
5. Kaech SM, Whitfield CW, Kim SK: **The LIN-2/LIN-7/LIN-10 complex mediates basolateral membrane localization of the *C. elegans* EGF receptor LET-23 in vulval epithelial cells.** *Cell* 1998, **94**:761-771.

6. Folsch H, Ohno H, Bonifacino JS, Mellman I: **A novel clathrin adaptor complex mediates basolateral targeting in polarized epithelial cells.** *Cell* 1999, **99:**189-198.
7. Brown DA, Rose JK: **Sorting of GPI-anchored proteins to glycolipid-enriched membrane subdomains during transport to the apical cell surface.** *Cell* 1992, **68:**533-544.
8. Scheiffele P, Peranen J, Simons K: **N-glycans as apical sorting signals in epithelial cells.** *Nature* 1995, **378:**96-98.
9. Yeaman C, Le Gall AH, Baldwin AN, Monlauzeur L, Le Bivic A, Rodriguez-Boulan E: **The O-glycosylated stalk domain is required for apical sorting of neurotrophin receptors in polarized MDCK cells.** *J Cell Biol* 1997, **139:**929-940.
10. Porter JA, Young KE, Beachy PA: **Cholesterol modification of hedgehog signaling proteins in animal development.** *Science* 1996, **274:**255-259.
11. Simons K, Ikonen E: **Functional rafts in cell membranes.** *Nature* 1997, **387:**569-572.
12. Brown DA, London E: **Functions of lipid rafts in biological membranes.** *Annu Rev Cell Dev Biol* 1998, **14:**111-136.
13. Cheong KH, Zacchetti D, Schneeberger EE, Simons K: **VIP17/MAL, a lipid raft-associated protein, is involved in apical transport in MDCK cells.** *Proc Natl Acad Sci USA* 1999, **96:**6241-6248.
14. Puertollano R, Martin-Belmonte F, Millan J, de Marco MC, Albar JP, Kremer L, *et al.*: **The MAL proteolipid is necessary for normal apical transport and accurate sorting of the influenza virus hemagglutinin in Madin-Darby canine kidney cells.** *J Cell Biol* 1999, **145:**141-151.
15. Lafont F, Lecat S, Verkade P, Simons K: **Annexin XIIIb associates with lipid microdomains to function in apical delivery.** *J Cell Biol* 1998, **142:**1413-1427.
16. Labouesse M, Hartwieg E, Horvitz HR: **The *Caenorhabditis elegans* LIN-26 protein is required to specify and/or maintain all non-neuronal ectodermal cell fates.** *Development* 1996, **122:**2579-2588.
17. Labouesse M, Sookhareea S, Horvitz HR: **The *Caenorhabditis elegans* gene *lin-26* is required to specify the fates of hypodermal cells and encodes a presumptive zinc-finger transcription factor.** *Development* 1994, **120:**2359-2368.
18. Nelson FK, Riddle DL: **Functional study of the *Caenorhabditis elegans* secretory-excretory system using laser microsurgery.** *J Exp Zool* 1984, **231:**45-56.
19. Perkins LA, Hedgecock EM, Thomson JN, Culotti JG: **Mutant sensory cilia in the nematode *Caenorhabditis elegans*.** *Dev Biol* 1986, **117:**456-487.
20. Ward S, Thomson N, White JG, Brenner S: **Electron microscopical reconstruction of the anterior sensory anatomy of the nematode *Caenorhabditis elegans*.** *J Comp Neurol* 1975, **160:**313-337.
21. Herman RK, Hedgecock EM: **Limitation of the size of the vulval primordium of *Caenorhabditis elegans* by *lin-15* expression in surrounding hypodermis.** *Nature* 1990, **348:**169-171.
22. Buechner M, Hall DH, Bhatt H, Hedgecock EM: **Cystic canal mutants in *Caenorhabditis elegans* are defective in the apical membrane domain of the renal (excretory) cell.** *Dev Biol* 1999, **214:**227-241.
23. Burke R, Nellen D, Bellotto M, Hafen E, Senti KA, Dickson BJ, *et al.*: **Dispatched, a novel sterol-sensing domain protein dedicated to the release of cholesterol-modified hedgehog from signaling cells.** *Cell* 1999, **99:**803-815.
24. Marigo V, Davey RA, Zuo Y, Cunningham JM, Tabin CJ: **Biochemical evidence that patched is the Hedgehog receptor.** *Nature* 1996, **384:**176-179.
25. Stone DM, Hynes M, Armanini M, Swanson TA, Gu Q, Johnson RL, *et al.*: **The tumour-suppressor gene *patched* encodes a candidate receptor for Sonic hedgehog.** *Nature* 1996, **384:**129-134.
26. Carstea ED, Morris JA, Coleman KG, Loftus SK, Zhang D, Cummings C, *et al.*: **Niemann-Pick C1 disease gene: homology to mediators of cholesterol homeostasis.** *Science* 1997, **277:**228-231.
27. Neufeld EB, Wastney M, Patel S, Suresh S, Cooney AM, Dwyer NK, *et al.*: **The Niemann-Pick C1 protein resides in a vesicular compartment linked to retrograde transport of multiple lysosomal cargo.** *J Biol Chem* 1999, **274:**9627-9635.
28. Gil G, Faust JR, Chin DJ, Goldstein JL, Brown MS: **Membrane-bound domain of HMG CoA reductase is required for sterol-enhanced degradation of the enzyme.** *Cell* 1985, **41:**249-258.
29. Nohturfft A, Brown MS, Goldstein JL: **Topology of SREBP cleavage-activating protein, a polytopic membrane protein with a sterol-sensing domain.** *J Biol Chem* 1998, **273:**17243-17250.
30. Collet J, Spike CA, Lundquist EA, Shaw JE, Herman RK: **Analysis of *osm-6*, a gene that affects sensory cilium structure and sensory neuron function in *Caenorhabditis elegans*.** *Genetics* 1998, **148:**187-200.
31. Legouis R, Gansmuller A, Sookhareea S, Bosher JM, Baillie DL, Labouesse M: **LET-413 is a basolateral protein required for the assembly of adherens junctions in *C. elegans*.** *Nat Cell Biol* 2000, **2:**415-422.
32. Scheel J, Srinivasan J, Honnert U, Henske A, Kurzchalia TV: **Involvement of caveolin-1 in meiotic cell-cycle progression in *Caenorhabditis elegans*.** *Nat Cell Biol* 1999, **1:**127-129.
33. Yochem J, Tuck S, Greenwald I, Han M: **A gp330/megalin-related protein is required in the major epidermis of *Caenorhabditis elegans* for completion of molting.** *Development* 1999, **126:**597-606.
34. Sym M, Basson M, Johnson C: **A model for Niemann-Pick type C disease in the nematode *Caenorhabditis elegans*.** *Curr Biol* 2000, **10:**527-530.
35. McMahon AP: **More surprises in the Hedgehog signaling pathway.** *Cell* 2000, **100:**185-188.
36. Aspock G, Kagoshima H, Niklaus G, Burglin TR: ***Caenorhabditis elegans* has scores of *hedgehog*-related genes: sequence and expression analysis.** *Genome Res* 1999, **9:**909-923.
37. Kuwabara PE, Lee M-H, Schedl T, Jefferis GSXE: **A *C. elegans patched* gene, *ptc-1*, functions in germline cytokinesis.** *Genes Dev* 2000, **14:**1933-1944.
38. Capdevila J, Pariente F, Sampedro J, Alonso JL, Guerrero I: **Subcellular localization of the segment polarity protein patched suggests an interaction with the wingless reception complex in *Drosophila* embryos.** *Development* 1994, **120:**987-998.
39. Brenner S: **The genetics of *Caenorhabditis elegans*.** *Genetics* 1974, **77:**71-94.
40. Riddle DL, Brenner S: **Indirect suppression in *Caenorhabditis elegans*.** *Genetics* 1978, **89:**299-314.
41. Hodgkin JA, Horvitz HR, Brenner S: **Nondisjunction mutants of the nematode *C. elegans*.** *Genetics* 1979, **91:**67-94.
42. Yandell MD, Edgar LG, Wood WB: **Trimethylpsoralen induces small deletion mutations in *Caenorhabditis elegans*.** *Proc Natl Acad Sci USA* 1994, **91:**1381-1385.
43. Jin Y, Jorgensen E, Hartwieg E, Horvitz HR: **The *Caenorhabditis elegans* gene *unc-25* encodes glutamic acid decarboxylase and is required for synaptic transmission but not synaptic development.** *J Neurosci* 1999, **19:**539-548.
44. Mello C, Fire A: **DNA transformation.** In *Methods in Cell Biology.* Caenorhabditis elegans*: Modern Biological Analysis of an Organism*, vol. 28. Edited by Epstein HF, Shakes DC. San Diego: Academic Press, Inc.; 1995:451-482.
45. Chalfie M, Tu Y, Euskirchen G, Ward WW, Prasher DC: **Green fluorescent protein as a marker for gene expression.** *Science* 1994, **263:**802-805.
46. Kyte J, Doolittle RF: **A simple method for displaying the hydropathic character of a protein.** *J Mol Biol* 1982, **157:**105-132.